DESIGN OF A DYNAMIC RADIOISOTOPE POWER SYSTEM GENERATOR TESTBED

Ernestina Wozniak[1], Salvatore Oriti[1], Rebecca Buehrle[1], Ronald Leibach[1], Max Yang[1], Matthew Stang[1], Paul Raitano[1]

[1]NASA Glenn Research Center, Cleveland, OH, 44135

Primary Author Contact: (216) 433-3606, Ernestina.E.Schirmer@nasa.gov

The Dynamic Radioisotope Power System (DRPS) Testbed is a configurable laboratory test article designed to demonstrate the latest topology of a dynamic radioisotope power system generator. It utilizes an array of Stirling convertors arranged around a centrally located heat source that is radiantly coupled to the convertor hot ends. The Testbed is designed to dissipate all the waste heat through the housing and is outfitted with means for auxiliary cooling methods as well. During the past three years, the team at NASA's Glenn Research Center (GRC) has been designing and analyzing the various aspects of the DRPS Testbed. Currently, the parts for the Testbed are being manufactured, and the team is focusing on developing the test stand, supporting hardware, and assembly and operation procedures in preparation for the anticipated first operation of the DRPS Testbed in summer of 2022.

I. Introduction

For the past several decades, NASA has been investing in the development of dynamic energy conversion for powering space missions. Dynamic energy conversion enables power systems with higher conversion efficiency and more flexible choices for energy sources than the existing power systems used on current missions.

Two common types of power systems that have been flown on NASA missions are photovoltaic systems and thermoelectric-based Radioisotope Power Systems (RPS). A large disadvantage of using photovoltaic systems is there must be ample access to solar energy flux, which severely limits the environments where these systems can operate effectively. Thermoelectric conversion is significantly more flexible because it utilizes a nuclear heat source, Pu-238, to enable consistent spacecraft power without dependance on the environment. While thermoelectric conversion does provide increased flexibility, the latest thermoelectric-based RPS can achieve approximately 6% conversion efficiency as demonstrated by the recent Curiosity and Perseverance missions to Mars[1].

Dynamic power conversion is advantageous because it offers both high conversion efficiency, at least 20% end to end efficiency based on test data from the Stirling Research Laboratory (SRL) at NASA GRC, and environmental flexibility when integrated with a Pu-238 heat source. Despite the advantages, dynamic energy conversion has yet to be flown on a NASA mission. Recent developments in this area have demonstrated that dynamic energy convertors are in fact capable of the long-life, high-reliability operation necessary for even the longest missions to the outer planets. Additionally, the empirical test data gathered in NASA GRC's SRL shows zero-degradation of the convertors themselves, maximizing the available electrical power at the end of a long cruise mission, which is the most critical stage of the mission[2]. Further, several free-piston Stirling convertors operating in the SRL have demonstrated operational run times ranging from ten to fifteen years.

Most recently, technology development efforts have focused on demonstrating the heat engine conversion devices and understanding how to integrate them into a reliable and redundant power system. The latest topology for a DRPS generator utilizes free-piston Stirling-cycle convertors arranged in an array around a stack of general purpose heat source (GPHS) modules containing Pu-238, where the convertors are radiantly coupled to the heat source (see Figure 1). Redundancy is included in these concepts such that more Stirling-cycle convertors are incorporated into the designs than the minimum necessary to convert all the heat from the GPHS stack to electrical power. Each Stirling convertor, therefore, is nominally throttled to a lower level than its full design capability, allowing for a potential convertor failure, since the remaining units can be throttled up to maintain the total system power output.

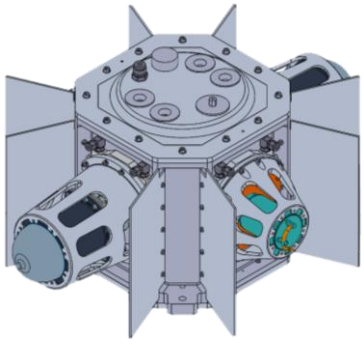

Fig.1. DRPS generator concept (external image of DRPS Testbed)

While this concept for a DRPS generator design has the advantages of efficiently capturing the heat from the GPHS blocks in addition to redundancy, it has yet to be attempted in a breadboard arrangement. To further investigate the concept and prove its viability, a specialized laboratory test article, the DRPS Testbed, has been designed.

The DRPS Testbed was conceived as a flexible test article, capable of operating with a range of Stirling convertor hardware, including legacy convertors from past projects as well as the most recent designs produced through NASA's DRPS project. The unique test article permits a range of experimental investigations that would not be possible with the other extended operation test setups that already exist in the SRL at NASA GRC. The most important aspects of investigation with the DRPS Testbed will include interactions and dynamics associated with operating more than one pair of convertors, radiant heat transfer from the centrally located heat source, and analyzing behaviors during simulated failure situations.

II. Requirements

The requirements for the DRPS Testbed were formulated with the goal of validating the proposed topology for a DRPS generator. The first requirement is that the Stirling convertors must be arranged in an arrayed layout with co-planar, dual-opposed pairs. Additionally, the DRPS Testbed must be capable of operating with either two or four Stirling convertors installed.

In the center of the DRPS Testbed must be a singular heat source that is radiantly coupled to the hot ends of the convertors. The heat source must be capable of simulating either two or three GPHS modules and must be of similar size and form to a stack of GPHS modules.

The housing of the DRPS Testbed must dissipate all the waste heat from the system and be capable of maintaining the cold end of the Stirling convertors at or below 100 °C in both ambient natural convection and in a thermal vacuum with a liquid nitrogen cold wall. There must also be provision for manipulating the cold end temperature independently of the natural convective cooling. Fins that are attached to the housing must be removable for conducting experiments with various fin sizes and materials.

Adaptability of the DRPS Testbed is required so that any available Stirling convertor in the SRL can be integrated into the system, including legacy Advanced Stirling Convertor (ASC) -E, -E2, and -E3 units, Stirling Radioisotope Generator Engineering Unit Stirling Convertor Assembly (SES) units, as well as the newer units delivered under the DRPS Project, Sunpower Robust Stirling Convertors (SRSCs) and Flexure Isotope Stirling Convertors (FISCs). The housing interior must have the capability to either be filled with up to 10 psig of inert cover gas or be evacuated. Finally, to account for a possible testing scenario where a single convertor is shutdown, there must include a place to attach passive balancers in the same axis as each convertor.

III. Design

The DRPS Testbed design started with determining the shape and approximate size of the main housing, then progressed to analyzing existing hardware and designing auxiliary components. Throughout each step of the design, thermal and structural analyses were performed to verify the functionality of each individual part. Once the design for the DRPS Testbed was finalized, the work transitioned to designing the test stand and support hardware.

III.A. Housing

The main radiator housing design began with an initial analysis of the required heat dissipation. Per the requirements, the housing and fins need to keep the cold ends of the Stirling convertors at or below 100 °C. Knowing the maximum thermal output from a GPHS block to be 256 W, the worst-case assumption was that the radiator would need to dissipate 80% of the total thermal output of the heat source. Additionally, the most thermal energy that the heat source would output is when it is simulating three GPHS blocks, resulting in 614.4 W as the maximum heat energy the radiator would need to dissipate.

Using the maximum heat dissipation required by the radiator housing, several shapes and configurations were analyzed in COMSOL to make an initial decision on the profile of the housing. In Table I. below, three external shapes were compared: octagon, circle, and square. Of those three, the octagon and circle were relatively similar in performance, but considering the hardware integration of the existing Stirling convertors, it is significantly easier to use flat instead of curved surfaces. Therefore, the decision was made to have an octagon shaped housing.

TABLE I. Comparison of housing shapes

Parameters	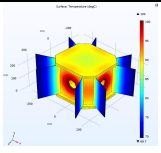	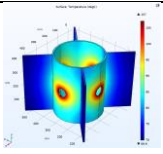	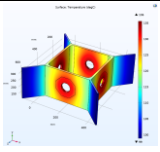
Shape	Octagon	Circle	Square
No. of fins	8	4	4
Total height	266.7 mm	406.4 mm	228.6 mm
Fin thickness	3.175 mm	9.525 mm	9.525 mm
Fin length	152.4 mm	177.8 mm	152.4 mm
Overall dia.	632.77 mm	684.29 mm	771.53 mm
Max. temp.	100 °C	107 °C	136 °C
Min. temp.	69.7 °C	69.9 °C	99 °C

The next comparison was to determine the ideal number and size of the fins and housing walls. Both thermal vacuum and ambient air simulations were performed in COMSOL, but since the radiator performed better in all cases under a thermal vacuum environment, the limiting environment is ambient air. A large number of cases were run with ambient air boundary conditions and variations on fin and wall thickness, height of the housing, and number of fins, and three cases are summarized in Table II below. It was desirable to have thinner fins, and eight fins would be much easier to integrate than twelve fins, therefore, the final design configuration was chosen to have eight fins and keep the fins thin as shown in Figure 2.

TABLE II. Comparison of octagon housing variations

COMSOL analysis	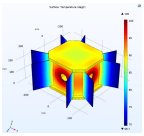	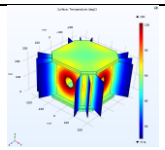	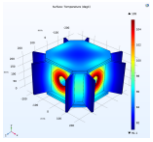
Shape	Octagon	Octagon	Octagon
No. of fins	8	12	8
Total height	266.7 mm	254 mm	241.3 mm
Fin thickness	3.175 mm	3.175 mm	12.7 mm
Fin length	152.4 mm	114.3 mm	120.65 mm
Overall dia.	632.77 mm	555.48 mm	564.71 mm
Max. temp.	100 °C	100 °C	105 °C
Min. temp.	69.7 °C	77.6 °C	91.1 °C

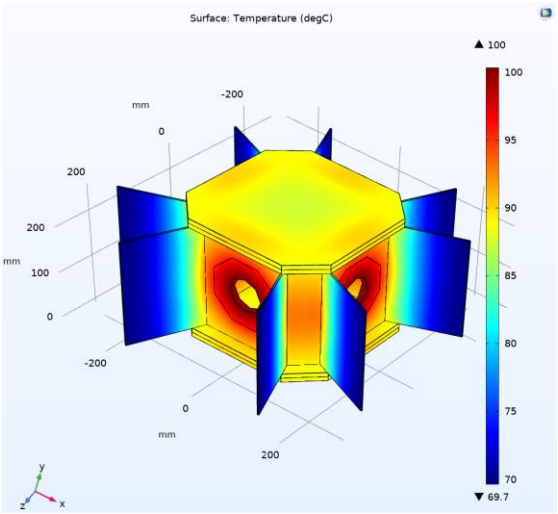

Fig.2. COMSOL analysis of initial housing design.

Structural analysis in ANSYS was performed on the housing to ensure that it would withstand the required conditions of an internal vacuum and pressurized to 10 psig. The results are summarized in Table III below. Maximum stress on the housing was lower than the yield stress of the 6061 aluminum housing material (38,000 psi) in both cases and was concentrated around the bolted joints, and the analysis indicated a safety factor of 1.5 for yield stress. Additionally, a modal analysis of the housing was performed, and Mode 1 frequency for both conditions was significantly higher than the standard operating frequency of the in-hand Stirling convertors.

TABLE III. Housing structural analysis

	Internal pressure of 10 psig	Internal vacuum
Stress plot	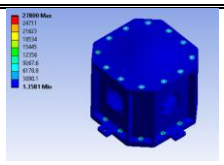	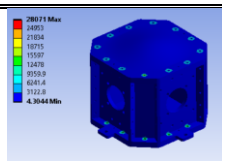
Max. stress	27800 psi	28071 psi
Deformation plot	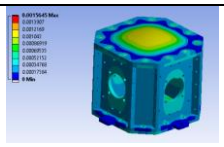	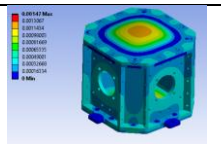
Max. deformation	0.00156 in.	0.00147 in.
Mode 1 frequency	310.42 Hz	316.92 Hz

The design of the housing was optimized after other features of the DRPS Testbed were defined and designed. Both the adapter plate (see the following section) and the cold-side adapter flange (CSAF) of the Stirling convertors have temperature drops, necessitating that these thermal resistances be accounted for to maintain the cold side temperature of the Stirling convertors at or below 100 °C. A COMSOL simulation analysis was performed on the adapter plates which indicated a drop across the plate of 2.4 °C. The radial temperature drop across the CSAF is more difficult to quantify due specialized material layering that is used during construction. While COMSOL simulations could have been performed, past studies have already quantified the radial temperature drop, specifically on the ASC-E3 CSAF design. This analysis indicates a maximum radial temperature drop of 14.7 °C (Ref. 3). Thus, it was determined that the maximum housing temperature had to be maintained below 82.9 °C, in order to achieve a cold-end operating temperature of the Stirling cycle below 100 °C.

Since the DRPS Testbed is designed to be operated with up to two pairs of convertors installed, and the heat source is designed to simulate either two or three GPHS modules, there are up to four potential operating conditions

while the convertors are operating in pairs. The first condition is with one pair of convertors stalled and the heat source simulating two GPHS modules. The second and third conditions are with all convertors operating and the heat source simulating two and three GPHS modules respectively. Finally, the fourth condition is with one pair of convertors stalled and the heat source simulating three GPHS modules. The fourth case would not be run during a real-world experiment because the heat input to the Stirling convertors would exceed their design limits, but it was included for a complete analysis.

Each condition was analyzed in COMSOL to ensure that the housing was able to dissipate the waste heat and keep the maximum temperature below 82.9 °C on the adapter plate interface surface for the three feasible conditions. For the purpose of this analysis, it was assumed that stalled convertors would parasitically conduct 30 W of heat per convertor, insulation losses would be 10% of the total thermal power of the heat source, and that the operational convertors would translate 20% of the heat input to the convertors into electricity. The results of these simulations are summarized in Table IV, and all the conditions, save the fourth unrealistic condition, were able to meet the temperature requirement, indicating that the housing design is sufficient to dissipate all the waste heat from the convertors.

TABLE IV. Housing operating conditions

	1	2	3	4
Simulation	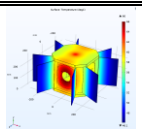	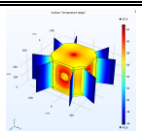	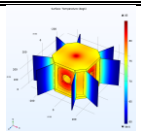	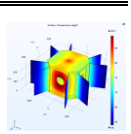
Heat source power	500 W	500 W	750 W	750 W
Insulation losses	50 W	50 W	75 W	75 W
Parasitic losses	60 W	0 W	0 W	60 W
Heat dissipated per convertor	156 W	90 W	135 W	246 W
Max. temp. on adapter plate	66 °C	60.7 °C	81.8 °C	89.2 °C

III.B. Adapter Plate

Due to the adaptability requirement, it was desirable for the DRPS Testbed to have minimal parts that were specific to the various Stirling convertors. To address this, the housing was designed to be symmetrical, but since the convertors that will be installed are not identical, and the GPHS module is not square, it was necessary to add an adapter plate to interface between the housing and the Stirling convertors. The adapter plates also serve several other purposes, namely: an internal coolant channel to provide auxiliary cooling, O-ring grooves on each side to seal between the housing and the Stirling convertors, and an octagonal clocking feature for maintaining convertor orientation through the CSAF interface during assembly (see Figure 3a).

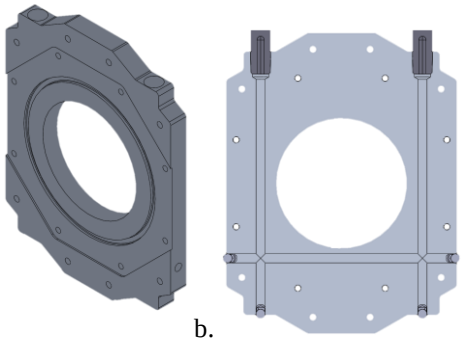

a. b.

Fig.3. a – Adapter plate with O-ring groove and clocking feature; b – Coolant channel in adapter plate

There are several dimensions that dictated the necessary thickness of the adapter plates (F in Figure 4). The critical dimensions are shown in Figure 4, namely: the distance between the CSAF and the hot end of the Stirling convertors (A), the thickness of the heat collector plate (B, discussed in the following section), the radiant spacing between the heat source and the heat collector plate (C), half the dimension of the heat source (D), the thickness of the housing (E), and the interior dimension of the housing (G). This allows for a simple equation to calculate the adapter plate thickness:

$$F = A + B + C + D - E - G$$

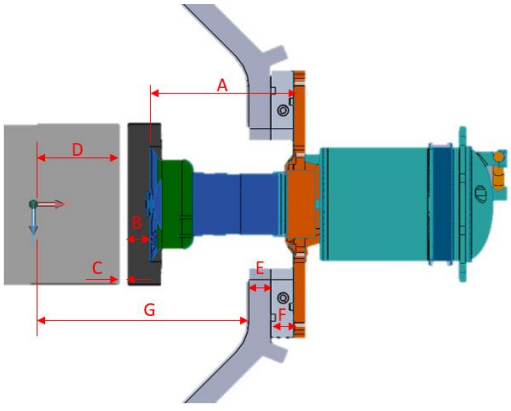

Fig.4. Critical dimensions for adapter plate sizing

The A dimension is fixed for each Stirling convertor, but differs for each convertor design. The B dimension was

also fixed to be 12.7 mm based on the heat collector plate design. Dimension C was determined to be 6.35 mm, the ideal dimension to keep the radiant view factor at approximately 0.9 for all faces of the heat source. Since the heat source resembles a stack GPHS blocks, and the GPHS block is not square, the D dimension depends on the orientation of the heat source. Housing thickness (E) was set to 12.7 mm so that there would be sufficient thickness for the blind, tapped holes necessary for mounting the adapter plates to the housing. Finally, the interior dimension of the housing (G) was calculated based off the convertor with the smallest A dimension, the smallest orientation of the heat source (D), and using a minimum adapter plate thickness of 12.7 mm to accommodate all the necessary features. Using all these defined factors, the thickness of the adapter plates (F) was determined for each Stirling convertor being utilized in the DRPS Testbed.

The coolant channel in the adapter plates is designed with three straight holes through the interior of the plate as shown in Figure 3b. Fittings are inserted in the top two ports, while the lower four ports are simply capped off with plugs. The channel was sized using heat transfer analysis and the heat transfer coefficient for each state of pump operation, baselining the Julabo Presto A40 circulator which is commonly used for testing dynamic energy convertors at NASA. After solving for Reynold's number for each pump state, the flow was found to be always turbulent. Using correlations with the Nusselt number for turbulent flow and the standard Nusselt number correlation shown in Equations 1 and 2 below[4], the heat transfer coefficient was found to be sufficient to dissipate all the waste heat from the DRPS Testbed for full cooling system redundancy.

$$Nu = 0.023 Re_d^{0.8} Pr^{0.4} \quad (1)$$

$$Nu = \frac{hD}{k} \rightarrow h = \frac{Nu \cdot k}{D} \quad (2)$$

Where Nu is Nusselt number, Re is Reynold's number, Pr is the Prandtl number, h is the heat transfer coefficient, D is the channel diameter, and k is the thermal conductivity of the coolant fluid. The quantified heat dissipation capability of the coolant channels is greater than necessary, which leaves a margin for the design.

III.C. Heat Collector

The hot ends of the Stirling convertors in the SRL are outfitted with circular expanders that are designed to interface with conductive heat sources. The DRPS Testbed, however, utilizes radiant coupling to the heat source, and the circular expanders are not ideal for radiant heat transfer from the rectangular faces of the heat source due to the low view factor and low surface area. To address this issue, heat collector plates were designed to expand the hot end of the Stirling convertors, and achieve a higher view factor. The heat collector plates are designed to be the same size as the faces of the heat source, and therefore, the standard governing equation for calculating the view factor for identical, parallel, directly opposed, rectangular surfaces was used and is shown in Equation 3 below[4].

$$F_{12} = \frac{2}{\pi XY}\left\{\ln\left[\frac{(1+X^2)(1+Y^2)}{1+X^2+Y^2}\right]^{\frac{1}{2}} + X\left(\sqrt{1+Y^2}\right)\tan^{-1}\left(\frac{X}{\sqrt{1+Y^2}}\right) + Y\left(\sqrt{1+X^2}\right)\tan^{-1}\left(\frac{Y}{\sqrt{1+X^2}}\right) - X\tan^{-1}(X) - Y\tan^{-1}(Y)\right\} \quad (3)$$

Where F_{12} is the view factor, X is a ratio of the longer side to the distance between the faces, and Y is a ratio of the shorter side to the distance between the faces. The view factor was calculated for a range of distances between the faces and plotted versus the distance between the faces as shown in Figure 5. It was desirable to have a view factor around 0.9, therefore a radiant spacing of 6.35 mm was selected.

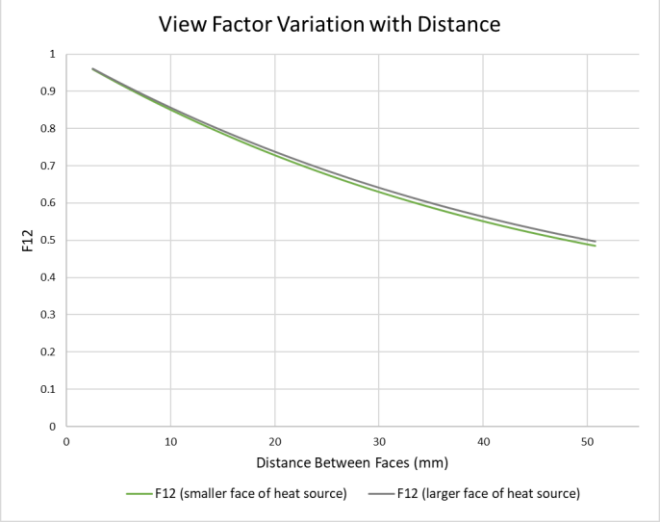

Fig.5. Variation of view factor with distance

The material for the heat collector plates was chosen to be Poco AXF-5Q graphite, which has excellent thermal conductivity and has been successfully used for past heat source designs in the dynamic energy conversion laboratory at NASA. The design was analyzed in COMSOL to ensure sufficient heat transfer and structural properties, and the results are shown in Figure 6a and 6b.

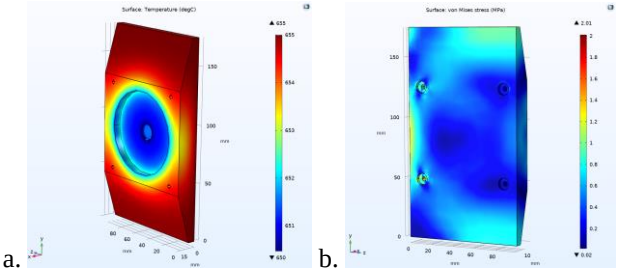

Fig.6. COMSOL analysis of heat collector plate: a – Conductive thermal analysis, b – Structural stress analysis

It was necessary to determine a method to attach the heat collector plates to the hot ends of the Stirling convertors without modifying the convertors. After iterating through several design ideas, the decision was made to use a spring-loaded draw rod system that mounts directly to the interior of the housing wall. As seen in Figure 7, each heat collector plate is supported by four draw rods, and each rod sits in a counterbore machined into the front surface of the heat collector plate. Then, at the end of each draw rod is a capture screw that encases a spring and a small end cap on the end of the draw rod. As the capture screws engage into the tapped holes in the housing wall, they compress the springs, providing an axial load that presses the heat collector plates onto the hot ends of the Stirling convertors. Due to concerns about creep life and thermal relaxation, it was necessary to choose springs made of a nickel-based alloy.

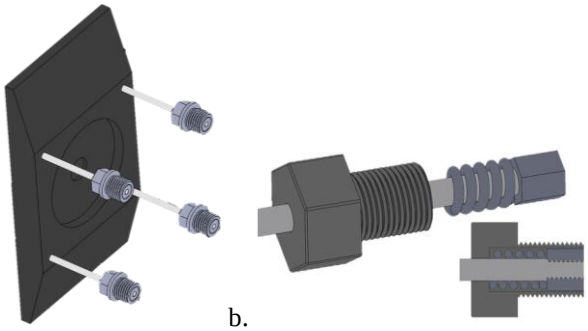

a. b.

Fig.7. a – Draw rod design; b – Capture screw mechanism

The draw rods were analyzed both thermally and structurally, and three possible materials were compared as shown in Table V. Per the analysis, the draw rods needed a tensile strength of at least 19.6 MPa. Based on this analysis, the decision was made to use Inconel for the draw rods because of the significantly better structural capability than either Macor or Rescor, despite the additional thermal losses.

TABLE V. Housing structural analysis

Material	Thermal loss calculated	Thermal loss simulated	Total loss from 16 draw rods	Tensile strength
Macor	0.113 W	0.118 W	1.896 W	32.9 MPa
Rescor	0.012 W	0.012 W	0.195 W	279 MPa
Inconel	0.883 W	0.924 W	14.779 W	980 MPa

III.D. Heat Source

The heat source for the DRPS Testbed resembles a stack of three GPHS blocks, but the thermal energy it generates can simulate either the output of two or three GPHS modules, satisfying the requirement. The design iterated through several options before settling on a simple option of a Poco AXF-5Q graphite block with through holes for inserting cartridge heaters, shown in Figure 8a. The cartridge heaters selected are Firerod heaters from Watlow and operate at temperatures up to 760 °C. COMSOL simulations were performed to determine the necessary heat source temperature and the temperature distribution across the block as shown in Figure 8b.

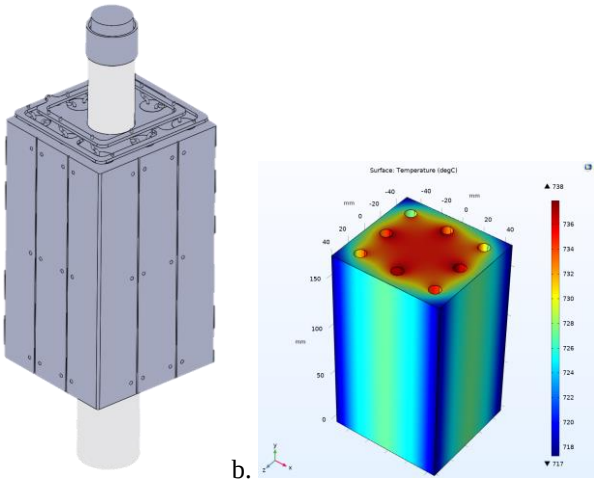

a. b.

Fig.8. a – Heat source block design with cartridge heaters installed, load studs, and spring assembly; b – Temperature profile of the heat source block

Several iterations of designs were considered for the heat source support before settling on a simple load stud design. The heat source is supported by two Rescor load studs, one on either side of the heat source (see Figure 8a). Each load stud is piloted via features in both the top and bottom end caps and the graphite heat source block. Again, COMSOL analysis was performed on the load stud to ensure that the performance requirements were satisfied. On the top load stud is a stack of Belleville washers that provide a spring force to support the heat source and hold it in place during operation.

III.E. Insulation Package

Inside the DRPS Testbed is a significant amount of empty space that needed to be filled with insulation. Multiple ideas for types of insulation to fill the space were considered, including a granular insulation that could be poured into place. Due to concerns with containing the grains and the assembly process, the decision was made to design an insulation package using microporous insulation instead, which has been used in insulation packages for extended operation of Stirling convertors at NASA. The DRPS Testbed insulation package consists of a series of separate interlocking pieces to fill the space and block line-of-sight losses (see Figure 9). Since some of the interior areas around the draw rod mechanisms are too small to be filled with microporous insulation, these areas will be filled with flexible blanket insulation.

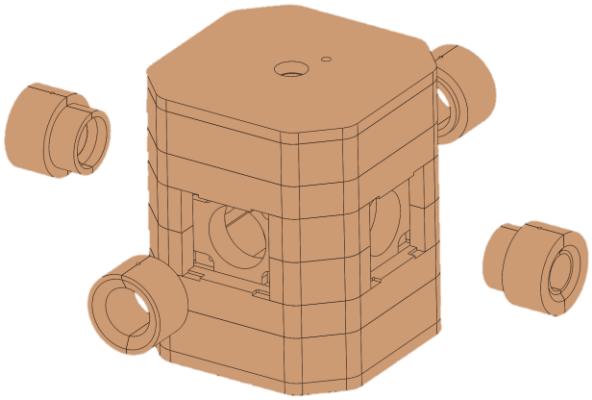

Fig.9. Insulation package design

III.F. Test Stand

One of the main aspects that will be investigated with the DRPS Testbed is the dynamics of operating multiple pairs of convertors simultaneously. The Stirling convertors are all mounted rigidly to the housing, but in order to fully isolate the system and detect any disturbances, it was necessary to design a mounting mechanism that floats the Testbed in the x, y, and z-axes. If the convertors are balanced perfectly, there would be no motion in any direction, therefore it is not necessary for the isolation mount to have large translation capability. The x-y-z isolation mount is pictured in Figure 10, and it consists of a series of plates and springs that allow motion in all three directions. The x and y-axes are isolated with the top two spring-plate systems, and the z-axis is isolated with springs encased in the feet that mount the system to the table. Any motion that is translated to the structure from the operating Stirling convertors will be detected and measured using an accelerometer.

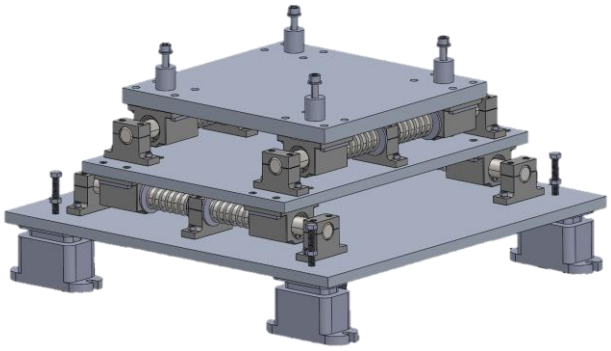

Fig.10. X-Y-Z isolation mount design

The other supporting hardware consists of a test rack, which was designed based on current and previous rack designs for tests performed in the SRL at NASA. All the current rack designs are only for operating either one or two Stirling convertors, so some modifications were necessary to allow for operation of four Stirling convertors, including designing a specific power panel and adding an additional fault protection circuit. The Stirling convertors will operate on passive DC bus control, which has already been demonstrated in the operation of FISC convertors. A channel list has been developed that will be used to develop LabVIEW software to operate the DRPS Testbed. Included on the list are all the parameters that will be recorded; measurements of voltage, current, and power for each convertor, various thermocouple measurements, heater parameters, and accelerometer readings are some of the key parameters that will be monitored.

IV. Current Status

The design work for the DRPS Testbed was initiated in early 2019. Over the past three years, the design has iterated through analyses and review processes to the current finalized state. In April 2021, a design review was held to present the design to project leadership at NASA prior to a peer review of the drawings for the Testbed which was held in August 2021. After the drawings were approved, they were sent to the manufacturing group at GRC. Some parts were sent out to an external vendor, while some are being manufactured in-house at NASA. All the parts are currently scheduled to be delivered by mid-April 2022, then assembly of the Testbed will begin. While the parts are being manufactured, the DRPS Testbed team is focusing on finalizing the design of the test stand, purchasing all the additional necessary components for assembly and operation, writing assembly and operational procedures, and preparing for a peer review of the test stand design in early April 2022.

V. Testing Plans and Conclusion

The DRPS Testbed activity was initiated to begin proving the viability of the latest generator topology, far in advance of any flight development project with a system integrator. The current flight DRPS contract with Aerojet Rocketdyne began the one-year design phase on December 22, 2021. If awarded the subsequent phase two option, the brass-board unit would be built and tested. The DRPS Testbed was designed with the ability to use in-hand legacy Stirling-cycle convertors and also maintains the ability to accept newer convertor hardware as they become available. Utilizing legacy, in-hand Stirling convertors reduced the cost of the DRPS Testbed and accelerated the first test to be possible as early as the summer of 2022.

The Testbed has four convertor installation ports and is flexible enough such that both pairs of Stirling convertors are not required to be the same design, even with entirely different sizes, masses, and voltage and power outputs. The DRPS Testbed will be used to evaluate various performance characteristics. Most significantly, the ability to radiantly couple the heat input zones of the thermodynamic cycles will be explored. This method of heat transfer may incur a larger thermal resistance link than a conductively coupled GPHS module and may also present additional thermal transients that need to be examined.

Additionally, the DRPS Testbed will be capable of independent operation of each convertor pair and evaluating convertor-level redundancy. One important test that will be conducted consists of disabling one pair of convertors and throttling the surviving pair up to 100% of the operational limits. Observations and responses will be recorded in all categories of interest: thermal, structural, and electrical.

The DRPS Testbed will also be conducive to thermal vacuum operation. The heat transfer characteristics have been designed to enable passive cooling both in ambient air and in an LN2-shroud environment. Also, the Testbed will at a minimum provide four spots for simultaneous extended operation testing on Stirling convertors, so it can potentially be utilized many years beyond the immediate need of demonstrating the latest DRPS generator topology.

The heat collector plate with the draw rod and capture screw mechanism employed to augment the hot end of each Stirling convertor is not known to be capable of launch vibration simulation, and this was not a requirement from the onset of the design activity. The mechanism may be capable, but more analysis is needed to determine whether running a vibration test is feasible. As such, there are no plans to perform any random vibration testing with the DRPS Testbed.

The DRPS Testbed forms a viable article to couple to flight-like, power-conditioning controllers, which are a critical subsystem of the DRPS. The controllers must modulate the load on the Stirling convertors to maintain their piston amplitudes, and they must also convert the alternator outputs to conditioned power usable by a spacecraft. In the laboratory setting this can be accomplished with the simple arrangement of a rectifier on the output of each alternator and then connected to a programmable DC load. In spaceflight, however, this must be performed by a much smaller and lighter set of hardware. The controller also has the duties of handling faults, both within its own components, and on the spacecraft electrical bus. In the latest topology for DRPS, the controller may also need to detect a failed convertor and implement a deliberate shutdown command to that pair. The Testbed will be coupled to in-hand and upcoming controllers to demonstrate the full end-to-end DRPS behavior.

The DRPS Testbed is an ideal laboratory test article to demonstrate a wide variety of concepts for DRPS generator systems. Adaptability was one of the key requirements of the Testbed design, and therefore the Testbed can be configured to test a wide range of conditions and analyze performance characteristics. The DRPS Testbed is an asset to future DRPS generator development efforts and will provide valuable testing capability for years to come.

ACKNOWLEDGMENTS

The DRPS Testbed is part of the DRPS project at NASA GRC. Special thanks also to Dave Gubics and Paul Schmitz for providing advice and experience to the team throughout the design phase, Mary Ellen Roth for logistical support, and Wayne Wong for supporting this effort.

REFERENCES

1. Multi-Mission Radioisotope Thermoelectric Generator (MMRTG), NASA, NF-2020-05-619-HQ, https://mars.nasa.gov/internal_resources/788/
2. N. A. SCHIFER and D. D. GOODELL, “Stirling Convertor Extended Testing in Support of Dynamic RPS Maturation”, *NETS 2020*, Virtural Conference, April 6-8, 2020 (2020)
3. G. MCNELIS and J. WHITE, “Thermal Test and Analysis of Press Fit CSAF-Transition Assembly” (2012)
4. F. P. INCROPERA, D. P. DEWITT, T. L. BERGMAN, and A. S. LAVINE, *Fundamentals of Heat and Mass Transfer*, 6th Ed., John Wiley & Sons, Inc., Hoboken, NJ (2007)
5. R. G. BUDYNAS and J. K. NISBETT, *Shigley’s Mechanical Engineering Design*, 9th Ed., McGraw-Hill Companies, Inc., New York, NY (2011)